# Uncertainty Analysis of a High-speed Dry Piston Flow Prover

Presented at 2002 Measurement Science Conference


**Harvey Padden**

**Bios International Corporation**
10 Park Place, Butler, NJ 07405, U.S.A.
973 492 8400 • Fax 973 492 8270
www.biosint.com • padh@biosint.com


PROVEN DryCal TECHNOLOGY

NVLAP Lab Code 200661

Bios
Driving a Higher Standard in Flow Measurement℠

## Abstract

This paper discusses a novel high-speed piston prover that uses a clearance seal to achieve very low uncertainties. We will review the instrument's design and provide an uncertainty analysis for three sizes of our internal reference provers, designed for flows of 10 ml/min to 50 L/min. Their expanded single-reading uncertainties at 2X coverage range from 0.064% to 0.073%. The instrument also has the capability to average a number of readings, potentially reducing the above uncertainies by a significant amount.

Traditional constant-displacement piston provers utilize mercury piston seals and low piston velocities. They have long been used as primary calibration devices for gases at low flow rates. Our design is based on our DryCal production design and it eliminates the seal.

The attraction of such a device is its combination of primary (dimensionally-based) flow measurement, simplicity and high speed and small size. However, this instrument has unique uncertainty sources that must be analyzed and controlled.

Uncertainty considerations for such a device include (among others) piston leakage, precise characterization of measured volume and the dynamics of a high-velocity underdamped free piston. Fortunately, the high speed of the device and the availability of a stable flow source allow sufficient data for a Type A analysis of the most significant uncertainties (75% to 88% of total u2).

## Introduction

There are a number of ways of characterizing low gas flows. These include constant-displacement provers, laminar flow elements (LFEs) and constant-volume (rate-of-rise) instruments. Our purpose was to develop a system for calibration of our production piston provers. For that reason, we desired an instrument of very high accuracy that is readily characterized by direct primary measurements. This discussion concerns the development of our primary laboratory provers.

Our goal was to develop volumetric instruments of 0.1 percent uncertainty. The readings were not to be standardized, but were to contain a small secondary correction for the pressure difference between the measuring cylinder and ambient.

This discussion concerns our master volumetric provers only. A separate analysis is needed for our production devices. We will concentrate our discussion on the unique areas of the analysis without discussing the straightforward areas in great detail.

Please note that these are volumetric provers for internal calibration of other, similar provers. This analysis covers the uncertainties associated with volumetric readings only. Standardization of the provers for other uses would incur additional uncertainties.

## Piston Prover Operating Principles and Variations

Constant-displacement systems are, perhaps, the simplest and most intuitive flow measurement devices. They have the extremely desirable characteristic of being characterized by the most basic of quantities: Length and time. As flow is necessarily a derived unit, a dimensionally characterized system would be as close as possible to direct traceability from national dimensional standards.

An idealized piston prover would consist of a massless, frictionless, leakproof, shape-invariant and impermeable piston inserted within the flow stream and enclosed by a perfect cylinder (Figure 1). The time that the piston takes to move a known distance (which implies a known volume) then yields the volumetric flow as:

$$F = V / T = \pi r^2 h / T$$

Such a device would be as accurate as its physical dimensions and its clock, with almost insignificant drift mechanisms. Of course, such idealized devices do not exist. Historically, three basic practical versions of piston provers have been employed.

## Bubble Devices

In their most basic form, piston provers can be nothing more than a calibrated burette within which a soap-film bubble rises with the gas flow. A stopwatch can be used to time the bubble's passage through a known volume between two marks. More modern bubble calibrators use optical bubble detection and an internal computer. The accuracy of any practical bubble device is limited by:

- Vapor pressure of water
- Shape variation of the bubble
- Permeability of the bubble
- Fluid viscosity changes with evaporation
- Variation of cylinder working diameter from dried and prior-reading bubble solution

The above-described uncertainties limit the usefulness of bubble devices. Vapor pressure alone can account for ±1.5% uncertainty. Bubble devices are of value when the insertion pressure must be as constant as possible, such as measurement of a very highly unregulated source.

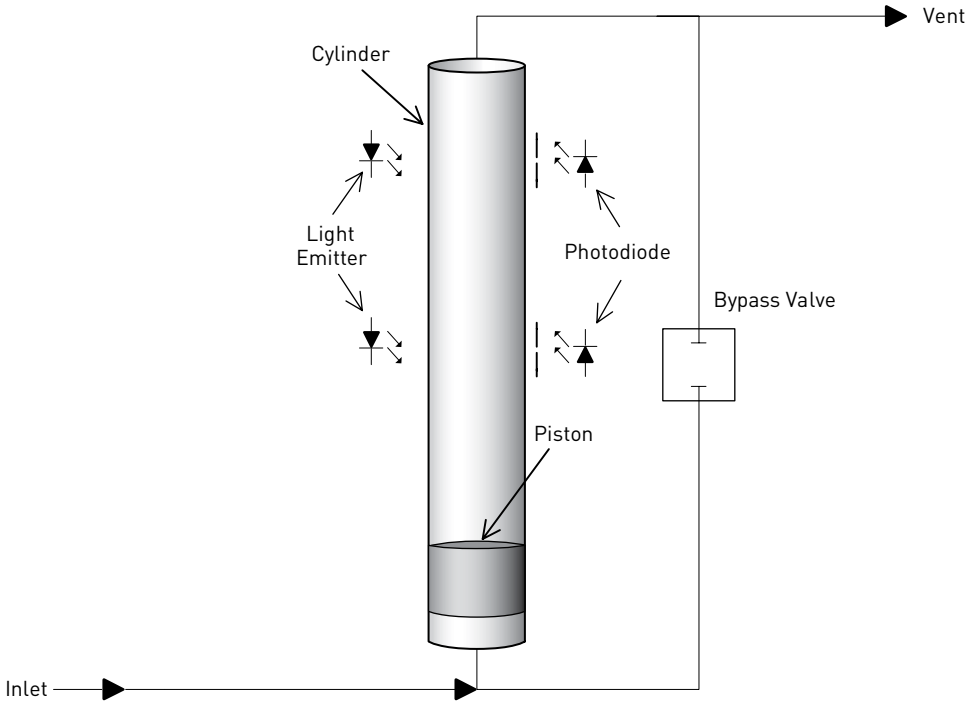


Figure 1 – Idealized Automatic Piston Prover

## Mercury-Sealed Provers

Mercury-sealed provers remedy some of the shortcomings of bubble calibrators. A rigid piston has the advantage of shape-invariability and impermeability, while gaining the disadvantages of requiring a seal and having a more significant piston mass.

In a laboratory calibrator used with high-stability flow sources, the piston mass can be made to cause minimal uncertainty. However, there is still the problem of sealing the piston. The best solution to date had been the use of a mercury piston ring to fill the gap between the piston and the cylinder. Its friction is very low and its vapor pressure is acceptable. However, piston speeds must be kept low to avoid loss of the mercury seal, limiting maximum flow rates and increasing measurement cycle time. A mercury seal also has the disadvantage of toxicity.

## Clearance-Sealed Provers

The DryCal clearance-sealed prover uses a piston and cylinder fitted so closely that the viscosity of the gas under test results in a leakage small enough to be insignificant. For reasonable leakage rates, such a gap must be on the order of 10 microns. As a practical matter, the piston and cylinder are made of graphite and borosilicate glass because of their low, matched temperature coefficients of expansion and low friction[1].

Such a device comes close to the ideal. The piston is shape invariant, impermeable and virtually frictionless. There is no vapor pressure from a bubble or sealant. The instrument can utilize high piston speeds, resulting in a measurement repetition rate rapid enough to be considered quasi-continuous.

An uncertainty analysis for such an instrument has unique considerations. The static uncertainties must be evaluated in a manner similar to that used for mercury-sealed provers. In addition, though, dynamic uncertainties resulting from a significant underdamped piston mass, the effects of enclosed dead volume and from leakage must be assessed.

## Detailed Description of a Clearance-Sealed Piston Prover (DryCal)

The actual provers analyzed here consist of two modules[2]. A base unit contains the power supply, computer, keyboard and display. An interchangeable measuring cell contains the entire pneumatic and sensor systems.

They are enhanced versions of our commercial DryCal ML-500, a ±0.35% instrument, shown in Figure 2. Three ML-500 measuring cells have been extended from 5 inches to 8 inches and the measured flow paths increased to 5 inches (small cell) and 4 inches (medium and large cells). Presently, the three cells cover the range of 25 mL/min to 50 L/min.

Figure 2 – DryCal ML-500

Each cell consists of a machined base containing the inlet and outlet fittings, bypass valve, temperature sensor and pressure tap. The bypass valve is of a self-relieving, low pressure, large area design. It latches in either the open or closed position to minimize introduction of heat into the flow stream. The pressure tap is located at the entrance to the measuring cylinder to maximize accuracy.

[1]U.S. Patent No. 5,440,925

[2]U.S. Patent No. 5,456,107

The base serves as a mounting for the vertical measuring cylinder/piston assembly, which uses a clearance-sealed piston to minimize friction. The cylinder is made of borosilicate glass and the piston is made of graphite. Both materials have a similar, very low coefficient of thermal expansion, allowing a precise fit to be achieved over a reasonable range of working temperatures. The effective cylinder diameter is neither the piston diameter nor the cylinder diameter: Rather, it is an intermediate value.

Detector slits are mounted directly to the cylinder's outer surface for maximum repeatability. A support structure is also attached to the base. It holds infrared light emitters and detectors, as well as the cell's electronic circuitry. Each cell contains all signal processing circuitry, A/D conversion and an EEROM for calibration data. In this way, complete calibration (with the exception of the computer's time base) can be performed on each cell individually.

A functional diagram of a DryCal piston prover is shown in Figure 3. Inlet gas ordinarily flows through the bypass valve to the outlet. When a reading is to begin, the bypass valve closes and the incoming gas displaces a piston that moves through a cylinder. After the piston has been allowed adequate time to accelerate, the time needed to pass from one optical sensor to another is measured. To the degree that the volume of the device is well known, we can derive the flow from measured primary dimensions (length and time).

Several additional elements of the practical design must also be considered. Temperature and absolute pressure sensors must be added to obtain standardized readings. The light detectors are collimated to increase accuracy. Finally, there is unavoidable dead volume consisting of the inlet fitting and tubing, interior passages, the valve and the portion of the cylinder below the point at which timing begins.

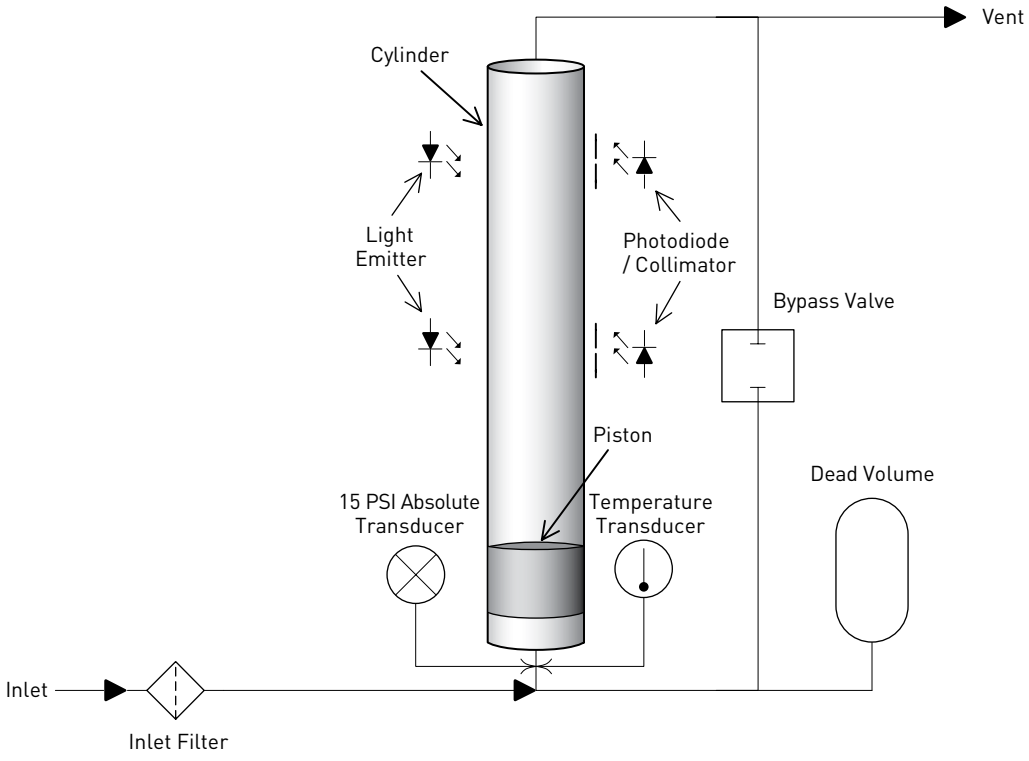


Figure 3 - Practical Piston Prover

## Sources of Uncertainty and Calibration Methods

The most important variables are piston diameter, measurement length (distance between encoder activation points) and time base frequency. These are calibrated by direct dimensional verification. Secondary variables with small uncertainty contributions are the effective piston diameter increase caused by the air gap, measurement length drift, leakage, pressure drop of the cell and thermal expansion.

## Measured Piston Diameter

The main precaution to be observed in measuring the piston diameter is to avoid deflection of the graphite piston by a measuring device. To avoid this problem, diameter is measured with a laser micrometer. Several readings are averaged to enhance accuracy.

## Effective Piston diameter

This subject is analyzed in detail in Appendix I. The following is a synopsis:

Direct measurement of the inside diameter of small cylinders over a relatively large distance is very difficult. For this reason, we use the instrument's internal self-test of the piston's leakage rate, the piston's weight and the viscosity of gas to calculate the maximum cylinder inner diameter using the Poiseuille-Couette equations (see Appendix I).

The aspect ratio of the gap is over 1000:1, so we can safely assume the flow within the gap to be laminar. Therefore, we know the effective diameter to be that of the piston plus the gap (½ of the gap X 2).

However, we cannot state with absolute certainty what the effective piston diameter is. Experimental data shows that the piston touches the cylinder tangentially during leakage tests. We use that condition as our nominal case

We can conservatively estimate the maximum effective diameter to be that of an elliptical piston of such eccentricity that it touches the cylinder at two points, but which yields the same leakage as the nominal case. Taking a ratio of the two yields our maximum effective diameter. Because the eccentricities are so small, the results are equally valid for an eccentric cylinder.

With similar reasoning, we can find the effective diameter for a tapered cylinder. The limit case is a cylinder that touches the entire piston circumference at one end, with the piston touching tangentially at all other points. This yields our minimum case.

We calibrate the instrument to a diameter between the tapered limit case and the elliptical limit case. Then, for conservatism, we can assume a maximum error of half the difference between the two cases with a u-shaped probability distribution.

## Measurement Length

The measurement length should be calibrated using the most representative method possible. The calibration is performed once the entire measuring cell is fabricated. The piston is positioned using a depth micrometer. The trip points actually detected by the mating optics and electronics are then used to determine the stroke length and its reproducibility.

## Leakage

Leakage will limit the instrument's accuracy at very low flows. The instrument is tested for piston leakage by raising the piston to the topmost position, sealing the inlet and timing the passage of the piston from the upper sensor to the lower sensor. The instrument then calculates flow rate by dividing the subtended volume by the time.

Since we know the piston's weight, the measured leak rate is also used to calculate the effective cylinder diameter (Appendix I).

## Dynamic Pressure Change

The DryCal is intrinsically a volumetric prover. As a piston prover is potentially subject to accelerative, oscillatory and piston-jamming effects, internal dynamic pressures must be measured to minimize uncertainty. To a first order, pressure only needs to be measured at the beginning and end of the timed measurement period. From the Ideal Gas Law, flow will be given by:

$$F = F_I\left[\frac{P_2}{P_A} + \left(\frac{P_2 - P_1}{P_A}\right)\frac{V_D}{V_M}\right]$$

Where:

$F$ = Flow

$F_I$ = Uncorrected Flow

$P_A$ = Ambient Pressure

$P_1$ = Pressure at start of timed period

$P_2$ = Pressure at end of timed period

$V_D$ = Dead Volume

$V_M$ = Measured Volume

Uncorrected, the measured volume contains an error equal to the difference in internal pressure at the start and the end of the measuring period, amplified by the ratio of dead volume to measurement volume, as well as that of the pressure within the cylinder at the end of the timed period. The DryCal is a high-speed device. As a result, the internal pressure changes rapidly and can significantly affect measurement uncertainty.

For this reason, true dynamic pressure measurement has been incorporated in this prover. Although an absolute pressure transducer could be used alone, additional sensitivity is gained and uncertainty reduced by using an additional sensitive gauge transducer summed with the absolute transducer (Figure 4).

Once the dynamic pressure correction is determined, it is used to correct for the potential uncertainty, thereby enhancing the instrument's accuracy. With knowledge of the dead volume, which will be constant for a given instrument design using a specified amount of external dead volume, the uncertainty resulting from the dynamic pressure differences can be minimized. This approach's effectiveness is limited by the pressure measurement's total accuracy (including secondary uncertainties such as synchronicity and quantization) and the dead volume's accuracy.

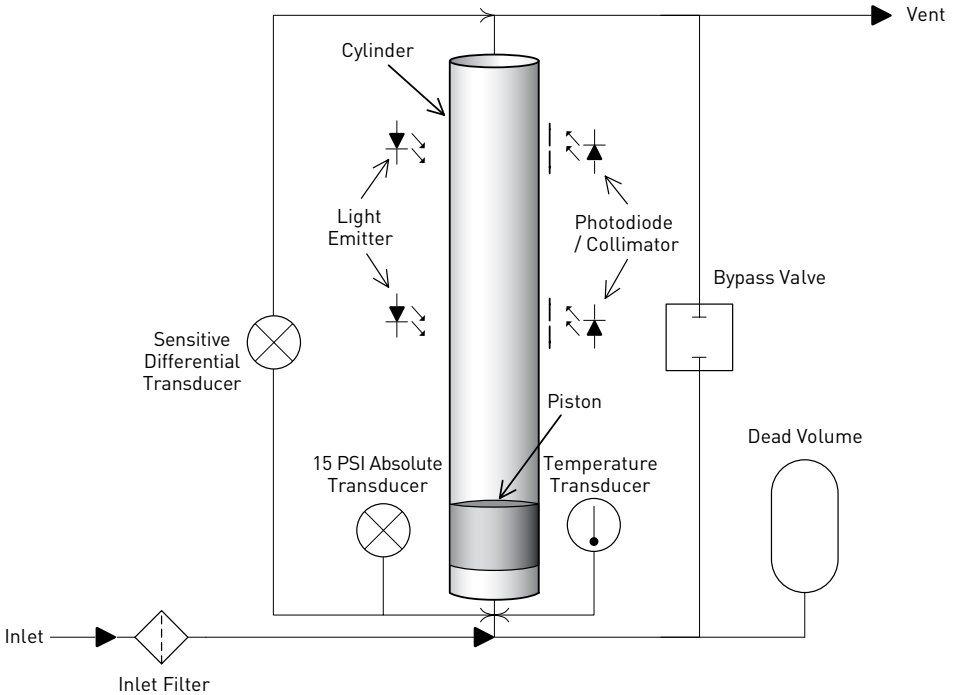


Figure 4 - Prover with Enhanced Dynamic Pressure Measurement

## Measurement Length Drift

Collimating slits attached to the glass cylinder's exterior mask the optical detectors. The effective width of the sensing slit is the actual slit width increased by the image of the emitter at the slit, reduced by any adaptive enhancement. The initial center-to-center spacing of the slits is a relatively straightforward measurement. However, significant potential uncertainty can arise from the position at which the sensor activates with respect to the slit. We must take into account the actual detector slit width, along with the size of the emitter's optical image at the detector slit (Figure 5).

The emitter is placed high enough to ensure that the light beam is always broken only by the edge of the piston furthest from the light source. This minimizes the geometric effect of the "optical lever" consisting of the distance from the piston edge to the sensor slit divided by the distance from the emitter to the piston edge. Specifically,

$h_e = H_e (d_s/d_e)$. The effective detector slit width is then $h_s+h_e$.

Calibration based upon direct measurement of the distances at which the piston is detected can eliminate these uncertainties, but there is potential for significant drift from other sources:

- Light output of the emitters can change with age, temperature and voltage.
- Detector sensitivity can change with temperature and age.
- Ambient light levels can change.

To minimize drift, we use an adaptive measurement scheme. Before each cycle, a reading of the ambient light level is taken for each photodiode with the light emitter turned off. Then a reading is taken with the light emitters turned on. An average of the two levels is then set as the trip level for that cycle. This is shown in Figure 6.

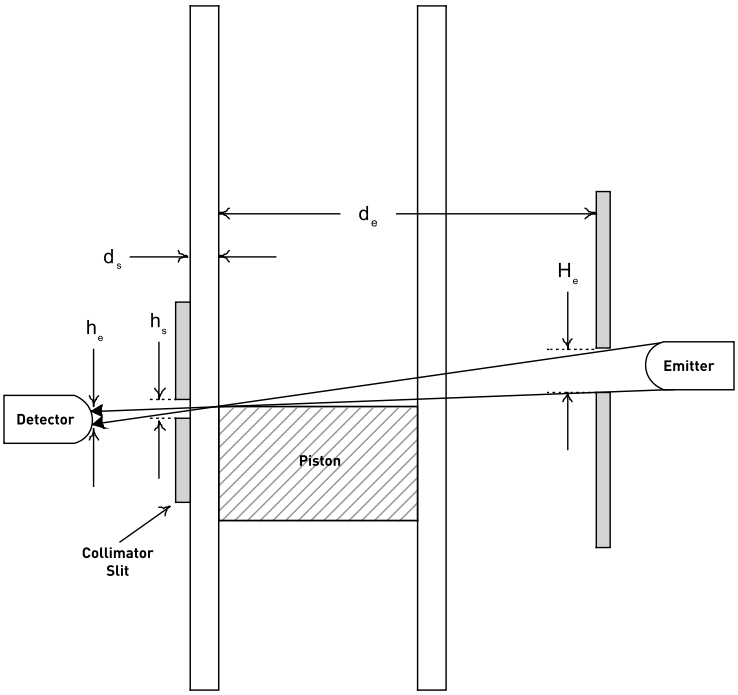


Figure 5 – Optical Geometry

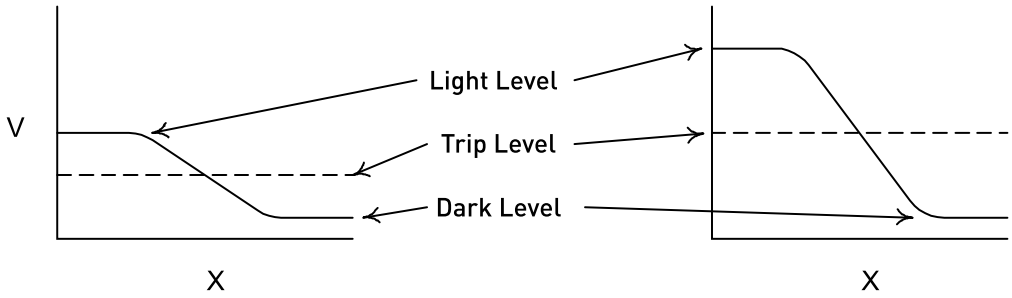


Figure 6 – Adaptive Detection

Using a fast A/D converter, we then measure the output of the photodiodes at intervals of approximately 150 microseconds during the piston's cycle of motion. We can reasonably assume that the geometry of the optical system does not change with time. Rather, the expected changes all affect the system's sensitivity. With a perfect A/D converter, we would then be able to eliminate all detector drift. For a practical converter, we will very conservatively assume a minimum signal level of 20 least significant bits (out of 4096 for our 12-bit converter). The effective detector slit width will then be the width calculated from the geometry previously described, reduced by a factor of 20:1.

## Piston Rocking

The piston can rotate about its center until its diagonally opposed edges contact the cylinder walls, causing an uncertainty in the height of the measured edge with respect to the center. However, quantitative analysis shows that the maximum uncertainty for these closely fitted pistons is less than 2 ppm.

## Thermal Expansion

The graphite piston and the borosilicate glass cylinder have similar thermal coefficients of expansion of approximately 7X10-$^{6}$/deg C. Over the maximum laboratory temperature range, specified as ±3 degrees Celsius, the maximum dimensional variation will be 21 ppm. This variation will apply to diameter and stroke length, resulting in a sensitivity coefficient of 3.

## Collection Time

### Time Base Calibration

The time base consists of a crystal oscillator that clocks the MCU's free-running 16-bit counter. A frequency counter is used to verify the crystal's rated accuracy of ±0.005%. The counter is applied after buffering to prevent probe errors.

### Timer Quantization

The photodetectors are adaptively measured every 150 microseconds. This process introduces a quantization error of ±75 microseconds. Since the measured time interval varies inversely with flow $(T = V / F)$, the quantization error is largest for the highest flow.

### Calculation and Display Quantization

Other quantization errors occur as a result of the display resolution and computer's internal divide subroutine. These errors are kept insignificant by designing to the proper degree of precision. The divide routine's resolution will be lowest at the highest flows, as it will be dividing a constant by a low time interval value.

## Values of Uncertainty Contributions

### Type A Uncertainties

**Reproducibility of Readings (Piston oscillations, rocking, detector trip point, quantization)**

Each of the three sizes of provers was connected to a stable flow source. After temperature stabilization, 100 readings were taken and analyzed for their standard deviation (including readout quantization). The results are tabulated in Table 1. It should be noted that this is a very conservative evaluation, as laboratory temperature changes and flow source changes are included in the resulting uncertainties.

Table 1 – Reproducibility of Readings

| Size | Flow (ml/min) | u | Maximum u |
|---|---|---|---|
| S | 30 | 0.032% | **0.032%** |
| S | 100 | 0.031% | |
| S | 200 | 0.019% | |
| S | 400 | 0.028% | |
| M | 100 | 0.020% | |
| M | 2000 | 0.027% | |
| M | 4000 | 0.030% | **0.030%** |
| M | 8000 | 0.026% | |
| L | 10000 | 0.029% | |
| L | 25000 | 0.034% | **0.034%** |

### Leakage

The reproducibility of leakage measurements was experimentally determined as described in Appendix I. The uncertainty was on the order of 14.9% of the leakage with a sensitivity of 1/3. This has an effect of less than 5% of the effective piston diametric uncertainty, making it statistically insignificant for diameter determination.

The leakage is, of course, very significant in determining the lower flow limit of the cells. The leakage itself was 0.05, 0.11 and 0.31 mL/min for the three cells. If we correct by adding the measured leakage from the readings, we still must contend with the leakage's uncertainty. This is approximately 0.0075, 0.016 and 0.046 mL/min for the three sizes. After the basic uncertainty analysis, we included the leakage uncertainty in a further, low-end analysis.

## Type AB and B Uncertainties

### Measured Piston Diameter

The average piston diameter was measured using a laser micrometer. Three diameters were measured by an accredited laboratory at 120 degree intervals at distances of one third and two thirds of the piston's height from one edge. The six readings were averaged to obtain the piston diameter. The expanded uncertainty stated by the measuring laboratory was 40 microinches.

Assuming a coverage factor of two, the uncertainty of the readings is 0.51 microns. Dividing by the piston diameters, we obtain uncertainties of 55, 22 and 11 ppm for the small, medium and large provers respectively. Since the volume is affected by the square of the diameter, the sensitivity factor is 2.

### Effective Piston Diameter

The effective piston diameter is the mean measured diameter plus one half of the annular gap as calculated in Appendix I. Its limit values are:

$$D = D_m + (0.685 \pm 0.160) \bullet \sqrt[3]{\frac{3F\mu h D_m}{wg}}$$

Where:

$D$ = effective piston diameter

$D_m$ = measured piston diameter

$F$ = Leakage flow rate

$\mu$ = viscosity of air

$h$ = piston height

$w$ = piston weight

$g$ = 980.7 cm/sec2

As the limit cases of taper and eccentricity cannot coexist, it is conservative to use a u-shaped distribution. Uncertainty is then:

$$u = \frac{0.160 \bullet \sqrt[3]{\frac{3F\mu h D_m}{wg}}}{D_m} \bullet \frac{1}{\sqrt{4.5}}$$

Effective piston diameter uncertainties are found in Table 2. Since the volume is affected by the square of the diameter, the sensitivity factor is 2.

Table 2 - Effective Diametric Uncertainties

| Size | Leakage (ml/min) | Diameter Correction | Variation (ppm) | u (ppm) |
|---|---|---|---|---|
| S | 0.039 | +0.049% | 113 | 53 |
| M | 0.11 | +0.023% | 51 | 24 |
| L | 0.31 | +0.016% | 36 | 17 |

### Measurement Length

The length of the timed stroke is determined by measuring the location optical detectors using a depth micrometer to move the piston. The location of each detector was measured separately. A number of readings were taken for each detector. Each reading reproduced the others within the digital micrometer's resolution of 0.0001 inches. Including the micrometer's rated accuracy and dividing by 1.732 for a rectangular distribution, we calculated the uncertainties of Table 3. The sensitivity factor is 1.

Table 3 – Detector Location Uncertainties

| Size | Detector | Tolerance (micro in.) | Distance | u (ppm) |
|---|---|---|---|---|
| S | Lower | 31 | 5.00 | 6 |
| S | Upper | 56 | 5.00 | 11 |
| M | Lower | 36 | 4.00 | 9 |
| M | Upper | 56 | 4.00 | 14 |
| L | Lower | 36 | 4.00 | 9 |
| L | Upper | 56 | 4.00 | 14 |

### Time Base

The time base is derived from a crystal rated at (and measured to) ±0.005%, or 50 ppm. Applying the appropriate factor for a rectangular distribution, $u$ = 50/1.732 = 29 ppm with a sensitivity factor of 1.

### Pressure Correction

In a volumetric device, correction of pressure to ambient is far less significant than in a standardized device. The uncertainty is that of the sensitive gauge pressure transducer when referred to the ambient pressure. In the small and medium sized cells, a full-scale pressure range of 2.5 cm water column is sufficient to measure the instrument's difference from ambient. For the large cell, 5 cm water column is necessary. Thus, the sensor system uncertainties are reduced by the ratio of full-scale pressure to ambient pressure, or approximately 0.0025 and 0.005 respectively. Over our limited laboratory temperature range of ±3 degrees Celsius, a simple silicon integrated transducer has a total uncertainty of less than 1%. The uncertainty of the absolute transducer is reduced by a similar ratio. Using a rectangular distribution, the combined uncertainty is 22 ppm for the small and medium provers, and 45 ppm for the large prover. The sensitivity factor is 1.

### Thermal Drift

The cylinder and piston have matched coefficients of thermal expansion of 7 X $10^{-6}$/ºC. Our laboratory temperature specification allows a tolerance of ±3 ºC. The resulting variation is ±21 ppm with a square distribution, so $u$ = 12 ppm. Expansion is in three dimensions, so the sensitivity factor is 3.

### Detector Drift

In addition to the measurement length uncertainty, we must also estimate the drift of measurement length with changes over time in sensor efficiency and emitter output. Although we are using an adaptive detection scheme, its efficiency is limited by quantization of the A/D converter. This, in turn, reduces the geometric uncertainty by a factor of ±½ bit divided by the number of bits difference between the light and dark levels, with a rectangular distribution. With our 4096 bit A/D converter, it is simple to assure that we have at least 20 bits of signal. This will reduce the geometric piston location uncertainty by a factor of 40:1, with a rectangular distribution. The individual uncertainty is multiplied by the square root of two to represent the two independent detectors. The resulting uncertainties are shown in Table 4.

Table 4 – Sensor Drift Uncertainties

| Size | Slit Image (inches) | Separation (inches) | Variation (ppm) | u Total (ppm) |
|---|---|---|---|---|
| S | 0.00079 | 5.00 | 79 | 64 |
| M | 0.0074 | 4.00 | 93 | 76 |
| L | 0.0069 | 4.00 | 87 | 71 |

## Uncertainty Statement

We base our uncertainty statement on the worst observed (Type A) reproducibility error for each cell size. Table 5 gives the maximum uncertainty for all but the lowest flows.

At the minimum flows, leakage uncertainty must be included. The expanded uncertainty remains below 0.1% for flows above 10, 25 and 80 mL/min for the three cells. The expanded uncertainties for the three cells at their lowest flows are shown graphically in Figures 7-9.

## Conclusions

This analysis leaves us confident that our goal of producing laboratory provers with uncertainties of less than 0.1% has been achieved. The calculated values of 0.064% to 0.073% should be conservative, as they include the uncertainties of the flow source and of the laboratory temperature. We also have confidence in the validity of the results because three quarters of the uncertainty is contained in Type A experimental results with 99 degrees of freedom.

There is also potential for reducing uncertainty by averaging multiple measurements. The DryCal has the capability for averaging multiple readings automatically. Its high, automated measurement speed makes this approach very practical. Although this approach would seem capable of halving the expanded uncertainty, we must remain cautious in its application. We must study the distribution of readings in our data for secular variations. Before blindly assuming from theory that averaging 10 readings will cut the reproducibility uncertainty by a third, we must perform verifying experiments.

We must also evaluate any long-term drift mechanisms not already accounted for. While experience from thousands of commercial DryCals shows that we do not have a significant wear mechanism, we need to be wary of such things as accumulated dust, for example. We will prepare two sets of the standards described, measure their internal intra-measurement pressures and compare them to each other periodically in an effort to establish a maintenance and calibration interval the minimizes such errors.

Other prospective future work includes:

- Performing the Type A repeatability experiments again with temperature correction. This should reduce our observed repeatability uncertainty. The DryCal ML design lends itself well to this approach, as it includes a temperature probe located directly in the flow stream, below the measuring cell.
- Performing data analysis to assess the degree of accuracy enhancement for different numbers of multiple readings. For example, a series can be constructed for running averages of $n$ sequential readings and its standard deviation calculated. Then a chart of $u$ versus $n$ can be prepared.
- Investigation of direct calibration of the cell volumes by gravimetric means (as a redundant test of our calibrations and to further reduce our uncertainty)

Finally, we will solicit inter-laboratory comparisons in order to further validate our results.

Table 5 – Uncertainty Statement

| SOURCE OF UNCERTAINTY | TYPE | Small u (PPM) | Med u (PPM) | Large u (PPM) | Sens. Factor | Small Net u (PPM) | Med Net u (PPM) | Large Net u (PPM) |
|---|---|---|---|---|---|---|---|---|
| **Reproducibility (99 d/f)** | A | 300 | 320 | 340 | 1 | 320 | 300 | 340 |
| **Measured Piston Diameter** | B | 55 | 21 | 11 | 2 | 110 | 42 | 22 |
| **Effective Piston Diameter** | B | 53 | 24 | 17 | 2 | 107 | 48 | 34 |
| **Upper Detector Location** | B | 6 | 9 | 9 | 1 | 6 | 9 | 9 |
| **Lower Detector Location** | B | 11 | 14 | 14 | 1 | 11 | 14 | 14 |
| **Time Base** | B | 29 | 29 | 29 | 1 | 29 | 29 | 29 |
| **Pressure Correction** | B | 22 | 22 | 44 | 1 | 22 | 22 | 44 |
| **Thermal Expansion** | B | 12 | 12 | 12 | 3 | 36 | 36 | 36 |
| **Detector Drift** | B | 64 | 76 | 71 | 1 | 64 | 76 | 71 |
| Total u (percent) | | | | | | 0.036% | 0.032% | 0.036% |
| Coverage Factor | | | | | | 2 | 2 | 2 |
| **Overall Uncertainty (percent)** | | | | | | 0.073% | 0.064% | 0.071% |

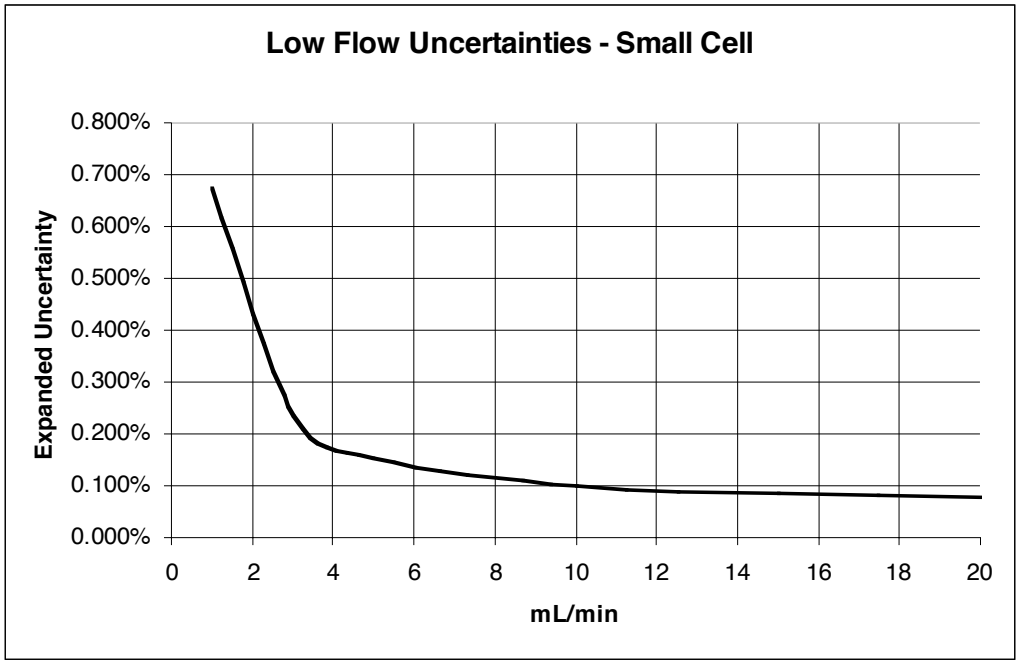


Figure 7 – Expanded Uncertainties at Low Flows (Small Cell)

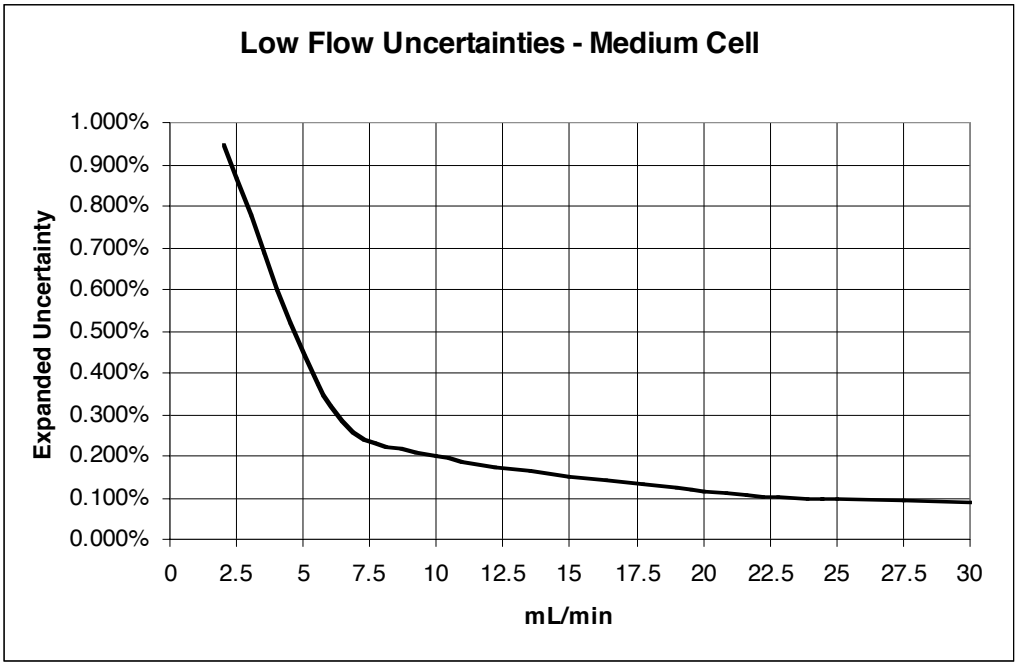


Figure 8 – Expanded Uncertainties at Low Flows (Medium Cell)

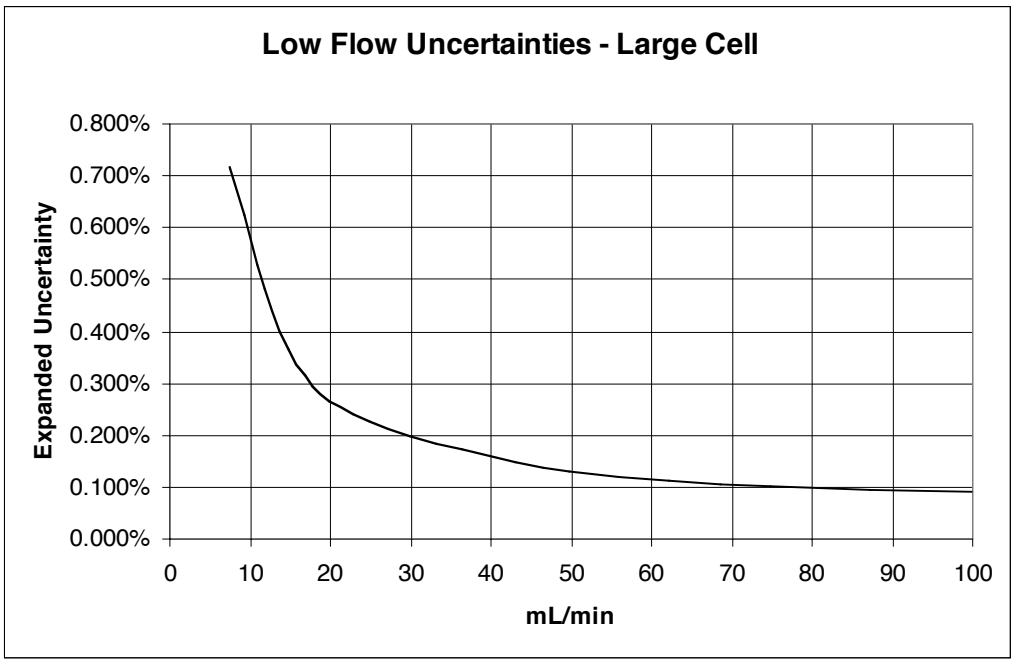


Figure 9 – Expanded Uncertainties at Low Flows (Large Cell)

## Appendix I:
## Derivation Of Effective Piston Diameter

The outer diameter of a cylinder can be measured more easily and precisely than the inner diameter of a cylinder. The instrument self-tests for piston leakage, so we can use the piston diameter, the leakage and the viscosity of air to find the effective average cylinder diameter. We can set a maximum effective piston diameter by treating the piston and cylinder as circular sections. Then we can set a minimum effective diameter by making conservative extreme-case assumptions about eccentricities and taper as part of a perturbation analysis.

## Concentric Cylinder Diameter From Piston Diameter And Leakage

Let us assume, at first, that the cylinder and piston are circular and concentric. The piston and cylinder can be treated as parallel plates of a width equal to the mean circumference and equal in height to that of the piston. Knowing the viscosity of gas and the maximum leakage, we can calculate the maximum gap (or annular ring thickness).

During the leakage self-test, the piston's weight exerts a pressure on the gas contained in the closed, lower portion of the cylinder. The piston sinks in the cylinder as a result of the leakage through its clearance seal. As the height of the piston is about 1000 times larger than the gap between the piston and cylinder, the leakage flow can be treated as laminar for our purposes.

The piston-cylinder interface can be treated as two parallel planes, one stationary and the other with a velocity. This devolves into a combination of Couette and Poiseuille flows. We can expect the Poiseuille flow to dominate: The annular gap area is expected to be a fraction of a percent of the piston area so the velocity of the gas in the gap should be hundreds of times that of the piston.

For combined Couette and Poiseuille flows, the flow, $F$, is given by:

$$F = W\left(V_p H - \frac{2H^3}{3\mu}\frac{dP}{dx}\right)$$

Where:

$W$ = Width of parallel surfaces

$V_p$ = moving plate or piston velocity

$H$ = half piston-cylinder clearance distance

$\mu$ = dynamic viscosity

For our purposes, this can be restated as:

$$F = W\left(\frac{V_p d}{2} - \frac{d^3}{12\mu}\frac{P}{h}\right)$$

Where:

$d$ = piston-cylinder clearance

$h$ = piston height

Or, substituting the piston's circumference for $W$:

$$F = \pi D\left(\frac{V_p d}{2} - \frac{d^3}{12\mu}\frac{P}{h}\right)$$

Where:

$F$ = flow rate

$D$ = piston diameter

Substituting flow rate divided by piston area for $V_p$, we have:

$$F = F\left(\frac{4d}{D}\right) - \frac{\pi D d^3}{12\mu}\frac{P}{h}$$

Since we know d to be on the order of 10 microns, the first term (representing the Couette component) will be very much smaller than unity and can be safely ignored. This is as we expected from our initial observation of the great difference between the piston and flow velocities. Now our equation devolves to:

$$F = -\frac{\pi D d^3}{12\mu}\frac{P}{h}$$

Solving for the annular gap, d, yields:

$$d = -\sqrt[3]{\frac{12F\mu h}{\pi DP}}$$

We can use the piston's weight and its area to substitute for pressure:

$$P = \frac{-4wg}{\pi D^2}$$

Where:

$w$ = piston weight

$g$ = 980.7 cm/sec2

Finally yielding:

$$d = \sqrt[3]{\frac{3F\mu hD}{wg}}$$

## Experimental Observations

Our first test was to find the standard deviation of the leakage and to determine whether the position of the piston during the leak test is generally tangential, with the piston contacting the cylinder.

The cylinder was placed at an approximate angle of 5 degrees from the vertical. Leakage rates were then measured at each of 18 equally spaced angles when viewed vertically. In other words, the leakage readings were distributed evenly about a cone at 5 degrees from vertical. In addition, 8 readings were taken with the cylinder in the vertical position.

The first, angled, series of measurements was designed to force the piston into contact with the cylinder such that they would form tangentially contacting cylinders. This yielded a mean leakage rate based upon the tangential (non-concentric) condition.

The series of measurements was made to find the mean leakage rate in the vertical position. This rate was similar to the rate in the non-vertical series. As there is a significant difference in the leakage rate in the concentric and tangential conditions, we can conclude that the leakage test always yields results consistent with the tangential condition. We should note that this test is only for determination of leakage and effective diameter: The piston can travel concentrically at high speeds, but this will not change the effective diameter.

These tests also allowed us to calculate the standard deviation of the leakage with sufficient degrees of freedom for validity. The standard deviation of the leakage readings was 14.9 percent. Since the leakage varies as the cube of the spacing, the standard deviation of the spacing as determined by the leakage test is 4.7 percent.

## Actual Cylinder Diameter From Piston Diameter And Leakage

There are three limit cases for a cylindrical piston and elliptical cylinder of equal cross-sectional areas. There is the idealized concentric case assumed in our original analysis. However, experiments show that the leakage is best described by a case in which the piston touches the cylinder. There are two such limit cases: Tangential and elliptical (Figure 10).


Figure 10 – Limit Cases of Equal Piston Area

It was now necessary to correct the idealized equations made for concentric cylinders for the tangential condition that we had found to be the actual geometry. We obtained a correction factor by:

1. Integrating the cube of the distance between two closely spaced tangentially touching circles. The dimensions were typical of those used in each of the three piston sizes.

2. Integrating the cube of the distance between two concentric circles of the same size.

Calculating a correction factor as the cube root of the ratio of the two values. This value was identical for all three cases: 0.736

Now we have obtained a corrected equation for the average piston-to-cylinder spacing of tangential cylinders as:

$$d = 0.736 \bullet \sqrt[3]{\frac{3F\mu hD}{wg}}$$

Next, we can analyze the range of effective cylinder diameters. Two deviations from dual tangential circular sections form our limit cases and are discussed below.

### Cylinder and piston eccentricity

Since the piston is on the order of 1000 times the gap, any eccentricity in the cylinder or piston must necessarily be very small. Therefore, we can assume that piston or cylinder eccentricities are cumulative and interchangeable. We can also assume that the area of the resulting elliptical sections can be calculated from their average diameters.

We can represent the worst-case eccentricity by an eccentric piston that touches a perfect cylinder at two points on its major axis. Once again, integrating the cube of the spacing around the cylinder is compared with the concentric-cylinder case. This time, the resulting gap correction factor is 0.845 from the concentric case, as the piston is necessarily centered.

### Cylinder taper

We can perform an analysis for a tapered cylinder in a manner similar to the eccentric case. The limit taper would be such that a perfect piston would touch the cylinder at one end. Such a case yields an equivalent gap of 0.714 times the non-tapered non-eccentric case. This factor, unlike the elliptical one, does not prevent tangential contact of the elements and must, therefore, be applied to the already-corrected nominal value. Our lower limit case is thus 0.736 X 0.714, or 0.526 times the concentric cylindrical case.

### Effective Piston Diameter and Standard Deviation

Limit cases of taper and eccentricity cannot coexist. They are, in that sense, dependent. However, for conservatism we will use the limit cases of both conditions. Our range of gap sizes is then from 0.526 to 0.845 times the concentric cylindrical case. Because the limit cases cannot coexist, we can remain conservative using a u-shaped distribution. This yields our final equation:

$$D = D_m + (0.685 \pm 0.160) \bullet \sqrt[3]{\frac{3F\mu hD_m}{wg}}$$

Where:

$D$ = effective piston diameter

$D_m$ = measured piston diameter

$F$ = Leakage flow rate

$\mu$ = viscosity of air

$h$ = piston height

$w$ = piston weight

$g$ = 980.7 cm/sec2

We can test this equation with some representative values:

$F$ = 0.3 cc/min = 0.005 cc/sec
$\mu$ = 1.835 X 10-4 gm/cm-sec
$h$ = 1.2 cm
$D$ = 2.4 cm
$W$ = 6.7 gm

Applying these values to the above equation yields a gap of approximately 6 to 9 microns. This is consistent with measurements of the actual cylinder's minimum minus its matched piston's maximum of 7 microns.

Bios

**Bios International Corporation**
10 Park Place
Butler, NJ, USA 07405

Phone: 973.492.8400
Toll Free: 800.663.4977
Fax: 973.492.8270

www.biosint.com